Available online at www.sciencedirect.com
ScienceDirect
Polymer 48 (2007) 2345–2354
polymer
www.elsevier.com/locate/polymer

Understanding the decomposition and fire performance processes in phosphorus and nanomodified high performance epoxy resins and composites

Weichang Liu [a,1], Russell J. Varley [b], George P. Simon [a,*]

[a] *Department of Materials Engineering, Monash University, Wellington Road, Clayton, Victoria 3800, Australia*
[b] *CSIRO Molecular and Health Technologies, Clayton, Victoria 3168, Australia*

Received 7 July 2006; received in revised form 30 January 2007; accepted 12 February 2007
Available online 14 February 2007

Abstract

This paper investigates the decomposition mechanism and fire performance of high performance epoxy amine resins and laminate systems, using thermogravimetry (TGA), energy dispersive spectroscopy (EDS), cone calorimetry and Fourier transform infra-red spectroscopy (FTIR). Two different, commercially-important epoxy resins, tetraglycidyl methylene dianiline (TGDDM) and diglycidyl ether of bisphenol A (DGEBA) have been cured separately with diethyl toluene diamine (DETDA) and bis(4-aminophenoxy)phenyl phosphonate (BAPP) and their relative combustion performance has been examined and discussed in terms of their decomposition profile. This paper highlights the close relationship between char yields (TGA and cone calorimetry) and thermal decomposition with the peak heat release rate, highlighting the role of the condensed phase in minimizing combustion. The lower decomposition temperatures and higher char yields of the tetra-functional epoxy (TGDDM) are therefore seen to provide superior fire performance compared to the bi-functional (DGEBA) epoxy. FTIR shows that the decomposition occurs through initial cleavage of P–O–C bonds in preference to other covalent bonds, which allows dehydration and subsequent charring and/or chain scission. TGA demonstrated that the laminated systems did not show a significant difference to the neat resin systems, with respect to initial decomposition of the network and the thermal stability of the char layer. Nanoclay addition was also found to have little effect upon degradation and fire performance.

Keywords: Epoxy resin; Fire performance; Phosphorus

1. Introduction

The use of phosphorus based fire retardants as more benign, environmentally friendly replacement additives to potentially toxic halogen based fire retardants in epoxy thermosets has been widely studied [1–6]. In recent times, research has focused more upon the use of reactive phosphorus containing species which are incorporated directly into the chemical structure of the network [7,8]. This has the benefit of being able to achieve similar levels of improvement in fire performance while minimizing any deleterious impact upon mechanical and thermal properties most likely due to the molecular level dispersion within a polymer matrix. Phosphorus containing species are considered to be more environmentally benign because they improve fire performance by forming a char layer which prevents or minimizes the transfer of combustible species to the gaseous phase [9–12]. Understanding the decomposition mechanism and the formation of the char layer of the epoxy network is therefore critical to further improving the fire performance of epoxy networks. This fire retardancy mechanism contrasts with the action of traditional fire

* Corresponding author. Tel.: +61 3 99054936; fax: +61 3 99054934.
E-mail address: george.simon@eng.monash.edu.au (G.P. Simon).
[1] Present address: Unilever Research China, 3F, XinMao Building, 99 TianZhou Road, Shanghai, PR China.

0032-3861/$ - see front matter © 2007 Elsevier Ltd. All rights reserved.
doi:10.1016/j.polymer.2007.02.022

retardants which tend to act in the gaseous phase by (i) scavenging free radicals and terminating propagating reactions and (ii) through the dilution of the gaseous phase with non-combustible products. A particular advantage of phosphorus based fire retardants, in comparison to traditional halogenated fire retardants, is the reduction in toxic gas emissions [13,14].

The degradation mechanism of an epoxy amine network, whilst highly complex, can be broadly understood in terms of a two-step process, starting with dehydration and followed by chain scission. The first step, dehydration, produces unsaturation in the form of an alkene species and liberates water, regardless of whether decomposition is in an oxidative or non-oxidative environment [15]. Subsequent to this process, chain scission of the polymer backbone occurs, forming free radical species which lead to a competition between further chain scission/polymer decomposition and polymerization/char formation. The direction in which this balance is shifted is dependent on factors such as the chemical nature of the degradation products and the oxidative or non-oxidative nature of the atmosphere [15–17]. In the case of phosphorus containing systems, the P–O–C and P–C bonds are more susceptible to cleaveage due to their lower bond strength, and act as weak links during thermal degradation [18]. Cleavage of the phosphorus species occurs, which decomposes to phosphoric acid which in turn leads to char formation [19]. The reactive nature of the radical phosphorus species [9] ensures that charring of the network takes place and effectively ''fixes'' the carbon to the phosphorus, creating a thermally stable layer which prevents the transfer of combustible gases and therefore potentially reducing flammability. Hergenrother et al. [20] studied phosphorus based epoxy systems further reinforcing the catalytic role that the phosphorus species play in the formation of the char in the condensed phase. They reported that the phosphorus acts specifically as a catalyst to char formation, whilst not specifically being involved in the char layer, and that the oxidation state of the phosphorus also played a significant role in determining the improvement in heat release.

Whilst the use of phosphorus containing species demonstrates considerable promise for improving fire performance of high performance networks, taking advantage of other synergistic processes to further improve properties remains a challenge. The emerging science of nanocomposites therefore presents a possible avenue of further improved fire performance, in concert with traditional phosphorus containing species, by taking advantage of the potential synergistic effect of phosphorus–silicon species [21,22]. For example, it has been reported for polyamides, that nanoclays are able to improve the thermal stability of a phosphorus based char layer whilst promoting migration of the layered silicate to the surface during combustion, thereby synergistically improving fire performance [23]. Chiang et al. [24] used a sol–gel process to synthesize a phosphorus and silicon containing epoxy network which contained significant improvements in fire performance as determined by LOI and significantly higher char yields as determined by TGA compared to the pure epoxy resin. Liu et al. [22] also incorporated phosphorus and silicon species into the backbone of an epoxy based network, through the use of phosphorus and silicone based diols. They reported that the LOI of the P/Si networks were synergistically improved over and above that observed for the P and Si only based networks due to an increase in the thermal resistance of the char layer. Recent studies have also shown that using the silicon species from a nanoclay can also result in a synergistic improvement in fire performance. Wang et al. [25] demonstrated that the activation energy barriers to degradation and the char yields at 450 °C were higher for phosphorus containing polyester nanocomposites, compared to the unmodified phosphorus containing polyesters. Chigwada and Wilkie [26] also investigated this synergy for polystyrene nanocomposites and found that the fire performance as determined using cone calorimetry and the UL-94 test, showed synergistic improvement when compared to the neat polystyrene. While the results showed some variability for the time to ignition, the clay and phosphate provided a very significant reduction in the peak heat release rate and the total heat released.

This paper presents research which seeks to understand the decomposition mechanism and its relationship to improved fire performance for a phosphorus based aromatic diamine hardener, bis(4-aminophenoxy)phenyl phosphonate (BAPP) and a non-phosphorus based hardener, diethyl toluene diamine (DETDA) cured with two different epoxy resins, namely diglycidyl ether of bisphenol A (DGEBA) and tetraglycidyl diamino diphenyl methane (TGDDM). Another aim of this work is to explore any synergistic improvements in either thermal stability or fire performance as a result of both nanoclay and phosphorus modification of the epoxy network. Comparison has also been made on any differences in behaviour between the neat resin sample and the carbon fibre reinforced laminate containing the modified resin systems. Experimental techniques used in this work include thermogravimetric analysis (isothermal and dynamic), energy dispersive spectroscopy (EDS), Fourier transform infra-red (FTIR) spectroscopy, and cone calorimetry, whilst nanocomposite formation was confirmed using XRD diffraction.

2. Experimental

2.1. Materials

The epoxy resins DGEBA and TGDDM were obtained from Vantico, Australia, with epoxide equivalent weights (EEW) of 189.7 and 105.5 g/epoxide, respectively. The phosphonate hardener BAPP was synthesized and purified according to the method previously reported [27]. The diethyl toluene diamine (DETDA) is a mixture of two isomers of 3,5-diethyltoluene-2,4-diamine (75–81%) and 3,5-diethyltoluene-2,6-diamine (18–20%) and was purchased from Albemarle Co. (USA) and used without further purification. The structures of BAPP, DETDA, DGEBA and TGDDM are shown in Fig. 1. The nanoclay used in this work was the organo-modified polymeric layered silicate, Nanocor I.30, (Nanocor, USA). The organocation rendering the silicate compatible with polymer matrices is octadecylammonium.

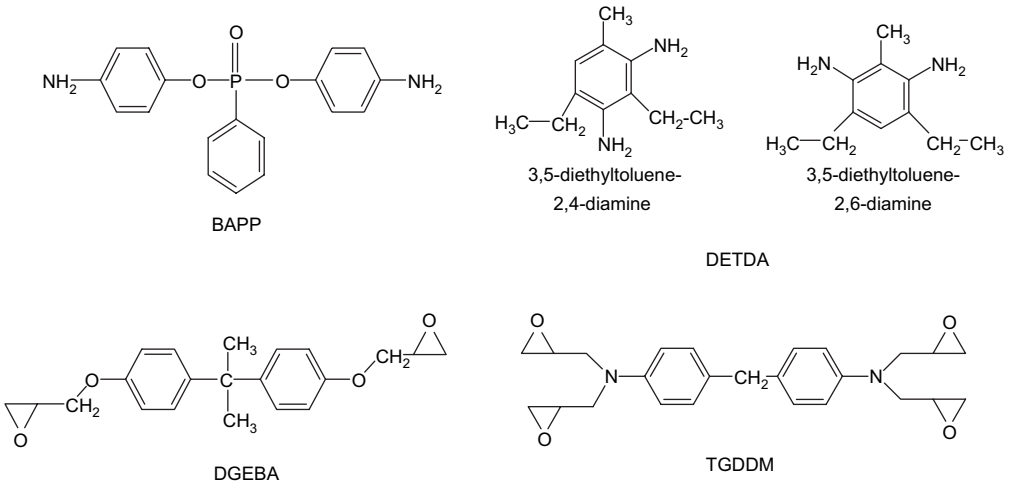

Fig. 1. Chemical structures of the compounds used in this work.

2.2. Sample preparation

2.2.1. Neat resin plaques

The curing agents were added to an epoxy resin in stoichiometric concentrations at 80 °C. They were mixed on a rotary evaporator until the system appeared to be free of bubbles. The resin was then poured into a pre-heated Teflon coated mould of dimensions 12 cm × 12 cm × 2.1 mm, and cured at 100 °C 2 h, 120 °C 2 h and 175 °C 4 h. A post-cure procedure was also carried out at 200 °C for 2 h. To prepare the nanocomposite systems, the nanoclay was added to epoxy resin prior to hardener addition at 80 °C, and the mixture vigorously stirred using a high speed mixer at 500 rpm for 1 h. The mixture was subsequently allowed to cool to room temperature, and the preparation continued, as discussed above for the neat resin systems.

2.2.2. Composite laminates

The reinforced laminates were fabricated by a hand lay-up procedure and then cured according to the same cure profile, except that the laminate was placed in a platen press and pressure applied after an appropriate time to ensure laminate consolidation. The known quantity of resin was manually spread out onto a section of plain weave carbon. The impregnated fibre was cut into 8 cm × 15 cm × 15 cm sections and stacked on top of each other keeping the fibres in the same direction as each other and then placed in a platen press. Table 1 lists the resin and composite systems prepared as part of this investigation.

2.3. Characterization

2.3.1. Thermogravimetric analysis

Dynamic thermogravimetric analysis was used to investigate the behaviour in an oxidative and a non-oxidative environment using a Mettler Toledo TGA/SDTA 851E instrument. For both air and nitrogen atmospheres a flow rate of 50 ml/min was used. Resin and laminate samples of approximately 15–20 mg were placed in the crucible and heated from 50 °C to 850 °C at a constant heating rate of 10 °C/min. Isothermal TGA was also performed using the same configuration, except that the temperature was held constant for 30 min at 330 °C, 360 °C, 410 °C and 500 °C for the resin systems only.

2.3.2. Fourier transform infra-red spectroscopy

A Bomem FTIR spectrometer was used to determine the chemical changes occurring during decomposition by using the samples that were isothermally degraded in the TGA. Spectra were recorded by preparing KBr discs, with particular attention being given to grinding the samples vigorously using a mortar and pestle. Spectra were taken over a range of 400–4000 cm^{-1} at a resolution of 7 cm^{-1} and the spectra were an average of 32 measurements.

2.3.3. Wide angle X-ray diffraction (XRD)

XRD was determined using a Rigaku Geigerflex generator with a wide angle goniometer. An acceleration voltage of 45 kV and a current of 22.5 mA were applied using Ni

Table 1
List of formulations prepared in this work for cone calorimetry evaluation and XRD results

Epoxy resin	Curing agent	Nanoclay (wt%)	*d*-Spacing[c] (Å)	Final form
DGEBA	DETDA	–	[a]	Laminate and resin plaque
DGEBA	DETDA	5	[b]	Laminate and resin plaque
DGEBA	BAPP	–	[a]	Laminate and resin plaque
DGEBA	BAPP	5	[b]	Laminate and resin plaque
TGDDM	DETDA	–	[a]	Laminate and resin plaque
TGDDM	DETDA	5	40.5	Laminate and resin plaque
TGDDM	BAPP	–	[a]	Laminate and resin plaque
TGDDM	BAPP	5	45.2	Laminate and resin plaque

[a] Not applicable.
[b] Beyond scale in instrument.
[c] Commercial nanoclay is 19.9 Å.

filtered Cu Kα radiation. The radiation wavelength was $\lambda = 1.540598$ Å.

2.3.4. Cone calorimetry

Cone calorimetry was used to investigate the combustion behaviour under ventilated conditions including time to ignition (TTI), rate of heat release (RHR), the maximum rate of heat release (PHRR), smoke density, carbon monoxide and carbon dioxide evolution. The heat flux used was 50 kW/m^2 on the specimen, which had an exposed surface area of 100 mm × 100 mm. Edge burning effects were reduced by covering the non-exposed sample surface in heavy duty aluminium foil. The device consisted of a radiant electric heater in a trunk-conic shape, an exhaust gas system with oxygen monitoring and instrument to measure the gas flux, an electric spark for ignition, and a load cell to measure the weight loss. All tests were terminated after 500 s of exposure. TTI measures the time to achieve sustained flaming combustion for a given cone irradiance. Smoke density was measured by the decrease in transmitted light intensity of a helium–neon laser beam photometer, and expressed in terms of specific extinction area (SEA), with units of m^2/kg. For RHR, the maximum value and the average to 180 s after ignition and the overall average values were determined.

2.3.5. EDS

Elemental analysis for C, N, O, Si, and P was determined on the degraded samples using Energy Dispersive Spectroscopy (EDS) with a Philips XL30 Field Emission Scanning Electron Microscope (FESEM).

3. Results

3.1. Nanocomposite formation

Wide angle X-ray diffraction was used to characterize the degree of nanoclay dispersion and intercalation/exfoliation in both the neat resin plaques, as well as in the composite laminates. Fig. 2 shows the traces for the DGEBA/BAPP cured resins and carbon fibre laminates which show that the ordering present in the layered silicates has been largely destroyed. This tends to suggest that either exfoliated or highly intercalated nanostructures have been formed in both the neat resin and laminate systems. Important to note also, is the similarity of the XRD traces between the laminate and neat resin plaques, suggesting that the laminate fabrication process did not interfere unduly with the formation of the nanocomposite. The corresponding raw traces for the TGDDM system (excluding the BAPP laminate) in Fig. 3 showed small peaks at values of 2θ of around 5° corresponding to d-spacing between the silicate layers of around 40–45 Å. A more ordered structure in the system compared to the DGEBA networks, suggests that the morphology is intercalated, rather than exfoliated. The values of the d-spacings for the neat resin systems as determined using XRD are also shown in Table 1. This decreased capability of TGDDM to exfoliate a nanoclay in comparison to DGEBA has also been reported by Becker et al. [28] for a similar system cured with DETDA, suggesting that nanoscale morphology is strongly influenced by the properties of the epoxy resin.

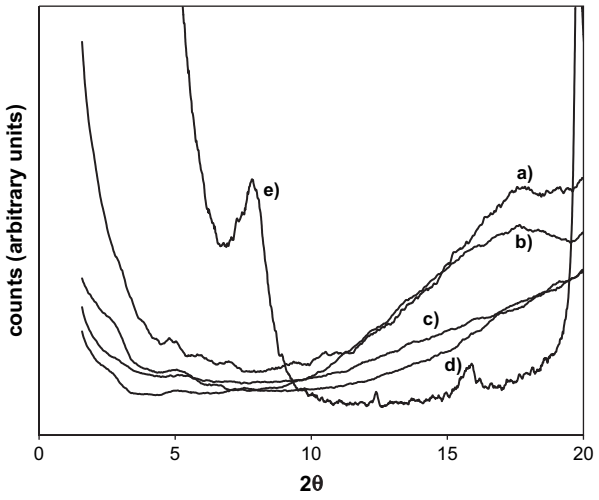

Fig. 2. XRD traces for DGEBA networks. (a) BAPP resin, (b) DETDA resin, (c) DETDA laminate, (d) BAPP laminate and (e) Nanomer I.28 organo-modified nanoclay.

3.2. Thermogravimetric analysis (TGA)

3.2.1. Dynamic scans

TGA was performed in dynamic mode for both the neat resin samples and the laminates, in an oxidative and a non-oxidative environment. The raw data traces for the DGEBA/BAPP and DGEBA/DETDA systems for the resin and the laminate systems under nitrogen and air are shown in Figs. 4 and 5, respectively. The non-oxidative degradation processes are made up of only one step (in the case of the DETDA system) or two steps (in the case of the BAPP systems), whilst the oxidative degradation processes contain approximately two

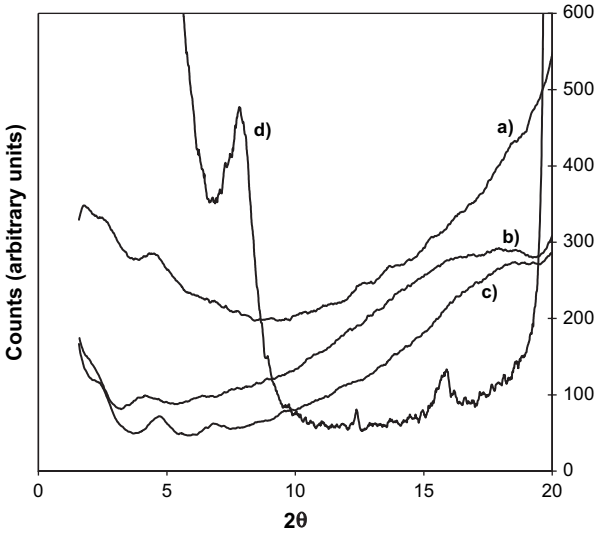

Fig. 3. XRD traces for TGDDM networks. (a) DETDA laminate, (b) TGDDM/DETDA, (c) TGDDM/BAPP and (d) Nanomer I.28 organo-modified nanoclay.

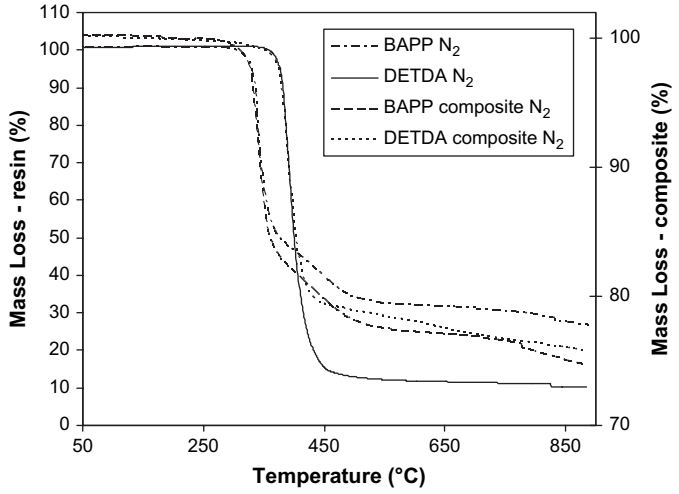

Fig. 4. Comparison of resin and laminate TGA traces for DGEBA in nitrogen.

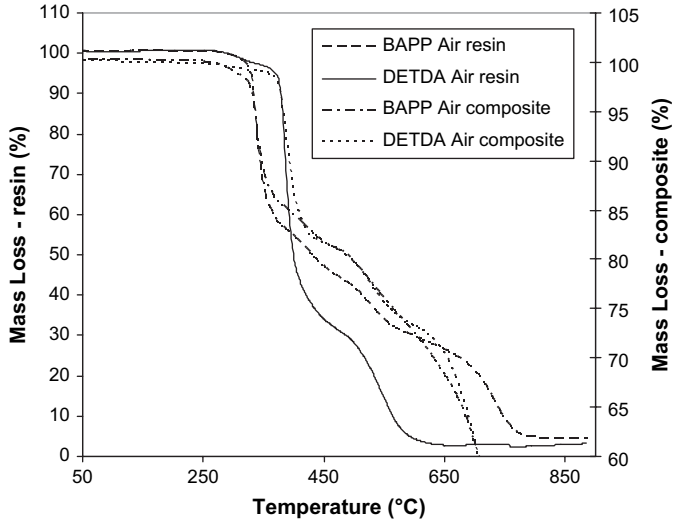

Fig. 5. Comparison of resin and laminate TGA traces for DGEBA in air.

steps (in the case of the DETDA systems) to about four steps (in the case of the BAPP systems). The char formed in a non-oxidative environment exhibits a high level of thermal stability beyond 450 °C up to at least 800 °C, and is substantially superior to the oxidative char yield. This illustrates the predominance of the char formation process occurring in preference to continued chain scission, in a non-oxidative environment. The presence of the phosphorus species can be seen to promote degradation through the lower onset of degradation temperature and higher char yields.

In the case of an oxidative environment, degradation is more complex. The char yields at 450 °C are higher compared to those in the non-oxidative atmosphere, yet at 800 °C the situation is reversed where the char yield is much lower than that in a non-oxidative atmosphere. This phenomenon is broadly observed for all of the samples measured, as shown in Table 2. This is again understood to arise from the competition between the crosslinking processes producing the char and continued chain scission. In this case, an oxidative environment clearly promotes the formation of a char layer earlier (i.e. the higher yield at 450 °C) and particularly in BAPP-containing systems, but they contain unsaturated functional groups rendering them more susceptible to further oxidation and chain scission as the temperature is further increased [15]. Also important to note from Table 2 is that the TGDDM systems display consistently higher char yields compared to DGEBA, whilst the thermal stability as measured via the temperature at 10% weight loss, tends to be lower than the DGEBA systems, despite being the more highly crosslinked network.

Comparison of the effect of carbon fibre reinforcement upon the degradation process, shown in Table 3, suggests

Table 3
First derivative TGA results for all of the samples prepared where the values refer to the temperature at the peak maxima

Sample	Nano-modifier (wt%)	Initial decomposition (°C)	Initial decomposition (°C)	Char decomposition (°C)
		Air	N_2	Air
DGEBA/DETDA	–	381.5 (386.4)	383.7 (388.5)	551.1 (527.9)
DGEBA/DETDA	5	385.0 (379.1)	379.0 (384.4)	565.7 (522.8)
DGEBA/BAPP	–	335.0 (332.8)	337.2 (336.6)	734.2 ([a])
DGEBA/BAPP	5	337.3 (337.2)	338.5 (340.7)	624.0 (583.3)
TGDDM/DETDA	–	349.6 (349.8)	351.2 (354.1)	583.2 (570.8)
TGDDM/DETDA	5	352.3 (352.9)	348.1 (355.1)	602.7 (543.8)
TGDDM/BAPP	–	315.6 (314.3)	312.5 (314.6)	713.7 ([a])
TGDDM/BAPP	5	318.5 (296.0)	318.4 (300.0)	667.5 (571.0)

Numbers in brackets refer to the degradation behaviour of the carbon fibre reinforced laminate.
[a] Peak unresolved from carbon fibre degradation peak.

Table 2
Results obtained from TGA showing the char yields at 450 °C and 800 °C and the temperatures corresponding to a 10% mass loss for all resin systems in both air and nitrogen

Sample	Nano-modifier (wt%)	$T_{10\%}$ (°C)	Char yield at 450 °C	Char yield at 800 °C	$T_{10\%}$ (°C)	Char yield at 450 °C	Char yield at 800 °C
		Air	Air	Air	N_2	N_2	N_2
DGEBA/DETDA	–	379.3	34.1	2.6	381.7	15.6	11.1
DGEBA/DETDA	5	379.3	32.6	5.6	372.3	19.8	14.3
DGEBA/BAPP	–	332.2	47.0	4.9	334.4	39.6	29.5
DGEBA/BAPP	5	336.3	47.4	12.5	336.5	40.8	32.6
TGDDM/DETDA	–	355.5	54.2	5.6	347.7	33.1	17.8
TGDDM/DETDA	5	348.1	50.9	7.2	337.4	35.5	23.5
TGDDM/BAPP	–	319.2	62.8	8.5	317.4	49.6	40.5
TGDDM/BAPP	5	318.4	61.4	12.3	316.2	49.2	39.5

that the same processes occur at similar temperatures, for either atmospheric condition. This indicates that carbon fibre does not have a significant effect upon the degradation process as measured using TGA. The addition of nanoclay can also be seen to have only a modest effect upon thermal stability. There is little effect upon the char yields at both 450 °C and 800 °C, while the thermal stability as measured by the temperature at 10% weight loss only decreases with the TGDDM/DETDA system. At 800 °C, increases in char yield were evident but merely reflected the level of inorganic additive present suggesting that no synergistic events were taking place. Fig. 6 shows the TGA of the first derivative spectra for the DGEBA-based networks in an oxidative atmosphere, which highlight the role of BAPP in determining network decomposition and thus indirectly the fire performance. The major peaks at below 350 °C, highlight the significant reduction in thermal stability of the cured network due to the more facile cleavage of the P–O–C bonds. The minor peaks at higher temperatures, however, show how the thermal stability of the char layer formed during decomposition is increased via significantly higher and broader transitions compared to the DETDA networks. This would therefore be expected to impact the fire performance if the fire retardancy mechanism is based upon the ability of the char layer to minimize the transfer of combustible gases to the gaseous phase.

3.2.2. Isothermal scans

Figs. 7 and 8 show the results of weight losses after 30 min at intermediate isothermal degradation temperatures for the DGEBA and TGDDM resin systems (excluding the DGEBA/DETDA/Nano and TGDDM/DETDA/Nano systems). Important points to note from this work which support dynamic TGA work are given below.

(i) The char yields for the phosphorus containing networks are substantially higher than the DETDA-based networks, regardless of the atmospheric conditions (apart from the initial decomposition temperature at 330 °C). This highlights the role of phosphorus in promoting initial decomposition.

(ii) There exists a transition temperature where the char yield in an oxidative environment drops below the corresponding char yield in the non-oxidative environment. This provides further evidence for the competing nature of the polymerization/char formation behaviour and the chain scission/polymer volatilization oxidation processes.

(iii) Comparisons of the char yields of the TGDDM/BAPP and DGEBA/BAPP systems, indicate that the char

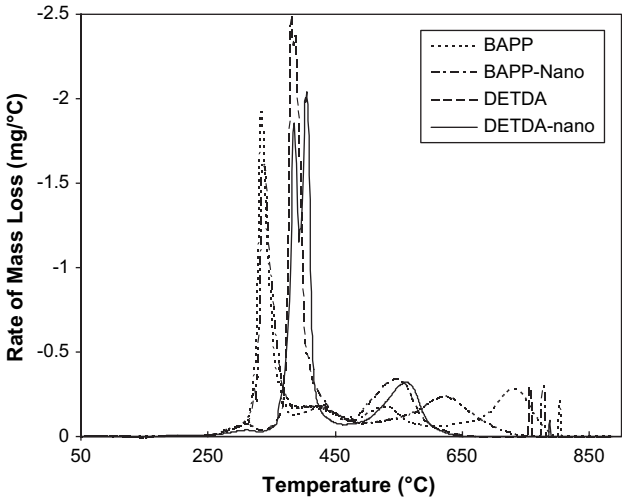

Fig. 6. First derivative TGA results for the DGEBA resin systems in air.

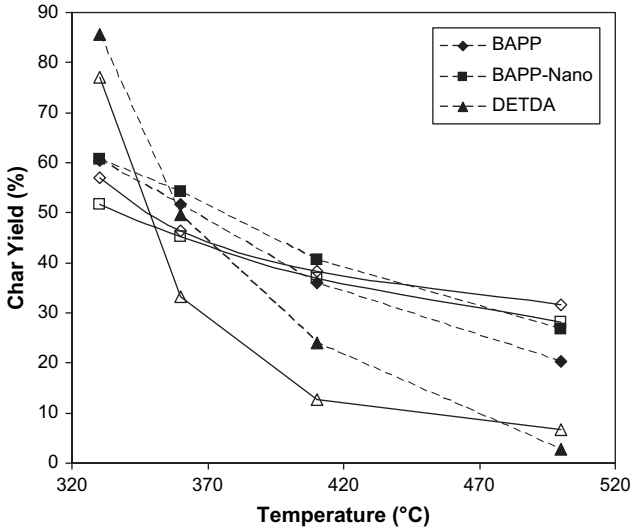

Fig. 7. Isothermal TGA for DGEBA/BAPP, DGEBA/BAPP/Nano and DGEBA/DETDA in both nitrogen and air atmospheres. (Open symbols and solid lines are for nitrogen atmosphere and closed symbols and dashed lines are for air atmosphere.)

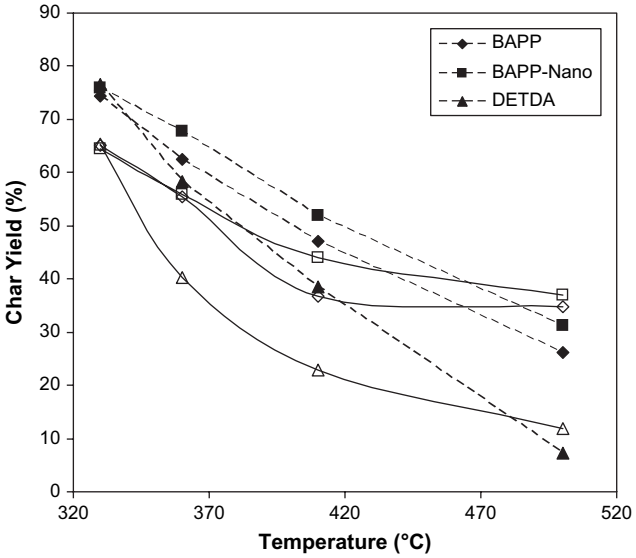

Fig. 8. Isothermal TGA for TGDDM/BAPP, TGDDM/BAPP/Nano and TGDDM/DETDA in both nitrogen and air atmospheres. (Open symbols and solid lines are for nitrogen atmosphere and closed symbols and dashed lines are for air atmosphere.)

yields for the TGDDM systems are higher than the DGEBA systems, supporting the dynamic TGA results.

3.3. Energy dispersive spectroscopy

Energy dispersive spectroscopy was used to measure the phosphorus and oxygen contents of the char residue prepared from isothermal degradation. The results are shown in Table 4 for the DGEBA/BAPP network, whilst Table 5 shows the results for the TGDDM/BAPP network. The normalized oxygen contents broadly display a depletion of oxygen content at lower degradation temperatures, which has been attributed to the dehydration process losing water (Rose et al. [29]) and H_2O and acetone (Levchik et al. [9]) and supports the proposition that initial degradation takes place via a dehydration step. At higher decomposition temperatures, however, both the TGDDM and DGEBA systems display an increase in the O/C ratio in an air atmosphere (oxidative environment) due to the formation of oxidation products. This is a reflection of increased levels of unsaturation and functional groups formed through such oxidation. In a non-oxidative environment, the O/C content displayed little change with increasing decomposition temperature, indicating improved thermal stability of the char layer in the absence of oxidation products. The TGDDM based nanocomposites show similar behaviour to the unmodified network, indicating that there was no increase in the resistance to oxidation as a result of nanocomposite formation. The changes in phosphorus (P/C) content with increasing decomposition temperature, also support these general conclusions. The substantially higher values of P/C in air compared to nitrogen show that the rate at which carbonaceous species are being lost to the gaseous phase is higher in an oxidative environment, compared to a non-oxidative environment, as would be expected. This highlights the lower thermal stability of the char layer and its susceptibility to further decomposition.

Table 4
EDS results showing the normalized oxygen and phosphorus compositions for the DGEBA resin system isothermally degraded in air and nitrogen

DGEBA/BAPP						
Temperature (°C)	O/C			P/C		
	Air	N_2	Air–nanocomposite	Air	N_2	Air–nanocomposite
RT	0.158	0.158	0.172	0.032	0.032	0.051
330	0.148	0.076	–	0.040	0.077	–
360	0.129	0.079	0.191	0.140	0.099	0.105
410	0.121	0.114	0.204	0.284	0.197	0.107
500	0.316	0.125	0.123	0.532	0.126	0.073

Table 5
EDS results showing the normalized oxygen and phosphorus compositions for the TGDDM resin system isothermally degraded in air and nitrogen

TGDDM/BAPP						
Temperature (°C)	O/C			P/C		
	Air	N_2	Air–nanocomposite	Air	N_2	Air–nanocomposite
RT	0.145	0.145	0.134	0.058	0.058	0.065
330	0.120	0.129	0.066	0.009	0.030	0.035
360	0.104	0.070	0.071	0.053	0.038	0.067
410	0.128	0.070	0.143	0.138	0.076	0.119
500	0.555	0.089	0.699	0.603	0.116	0.155

3.4. Fourier transform spectroscopy

The degradation mechanism was further investigated using FTIR spectroscopy on the samples that were isothermally degraded at varying temperatures. Fig. 9 shows the resultant spectra for the TGDDM/BAPP system degraded in an oxidative environment, whilst the corresponding samples for the DGEBA/BAPP network are shown in Fig. 10. The most

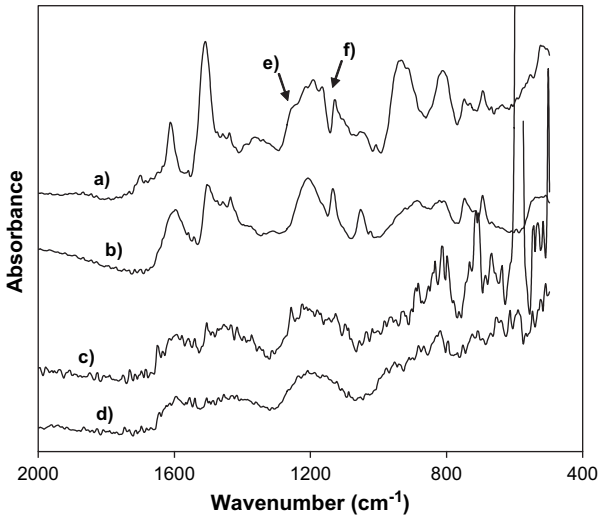

Fig. 9. FTIR spectra of the TGDDM resin samples isothermally degraded at increasing temperatures in an oxidative (air) atmosphere. (a) Undegraded, (b) 330 °C, (c) 360 °C and (d) 410 °C. (e) and (f) highlight the depletion of the P–O–C and P=O bonds with increasing decomposition.

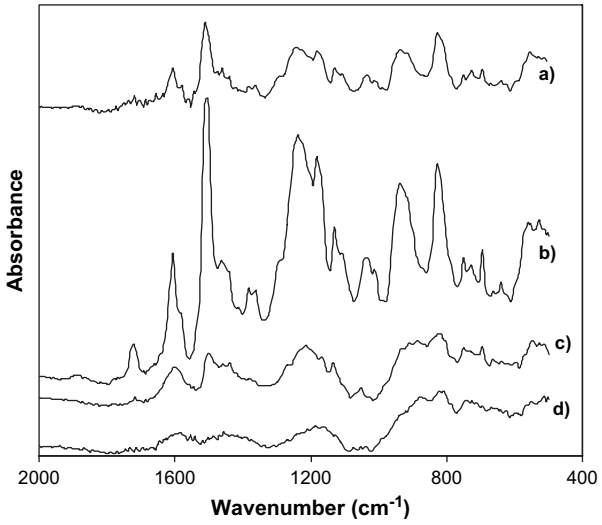

Fig. 10. FTIR spectra of the DGEBA resin samples isothermally degraded at increasing temperatures in an oxidative (air) atmosphere. (a) Undegraded, (b) 330 °C, (c) 360 °C and (d) 410 °C.

obvious effect of increasing decomposition temperature for both sets of spectra is the reduction in quality and the broadening of the peaks due to char formation. This is typical of FTIR spectra of degraded polymers, as reported elsewhere [17,18,30]. Given the extensive broadening of the peaks at the higher decomposition temperatures, the samples degraded at 330 °C are therefore the most useful in understanding the decomposition processes. Of particular interest are the bands associated with the P species, namely the P–Ph (1461 cm^{-1}), the P=O (1249 cm^{-1}) and P–O–C (1176 cm^{-1}) [18] absorption bands. Although it is difficult to determine the changes that these phosphorus containing bands undergo, it appears that for the TGDDM/BAPP network, the P–O–aryl bonds and the P=O are more reduced than the P–Ph bonds, as indicated in the spectra in Fig. 9 [denoted (e) and (f) in the figure]. In the corresponding DGEBA/BAPP spectra, there is less evidence of any disruption of these bonds, compared with the undegraded and degraded samples. This is in contrast to the work of Liu et al. [18] who cured a phosphorus containing epoxy resin (neither DGEBA nor TGDDM) with DDS and reported that the P=O and P–O–C absorption bands were not affected, but rather that the P–Ph which were cleaved in preference to the P–O–C bonds. The breadth of the aromatic peaks at 1608 cm^{-1} for both the TGDDM and DGEBA networks also indicated the presence of chemical changes at 330 °C. The peak in the TGDDM spectrum exhibits a significantly higher level of broadening compared to the DGEBA network, attributed to higher levels of unsaturation formed through dehydration. While this occurs to some extent for the DGEBA/BAPP network, it appears that a competing process which produces the carbonyl species (1728 cm^{-1}) also occurs decreasing the extent of dehydration for the DGEBA/BAPP network in air. As decomposition temperatures are increased, the carbonyl species is subsequently consumed, presumably due to ongoing degradation of the unsaturated species through oxidation and chain scission. In conclusion, we propose that the FTIR spectra provides evidence that the TGDDM/BAPP network displays a greater propensity for decomposition and char formation (and potentially improved fire performance), compared to the DGEBA/BAPP network. Specifically, the FTIR shows the following.

- Initial chain cleavage process of the P–O–C bond occurs for the TGDDM network, while competing processes are evident for the DGEBA/BAPP network.
- Increased unsaturation of the TGDDM/BAPP compared to DGEBA/BAPP is clear through the broader aromatic peaks at 1608 cm^{-1}.
- Increased levels of char are found for the TGDDM network, evident through the more rapid deterioration in the quality of the spectra with increasing decomposition.

These results and findings support those of Camino et al. [9,31] who suggested that the char is formed through a free radical polymerization process via unsaturated functional groups, or through the combination of the allylic radical species formed from the chain scission process.

3.5. Cone calorimetry

The fire performance of all samples was determined using cone calorimetry; the results obtained are presented in Table 6. For the cured resin systems, the peak and average heat release rates showed significant improvement for the

Table 6
Raw cone calorimetry data of all results for the systems studied

ID	Time to ignition (s)	Maximum rate of heat release[a] (kW/m^2)	Time to maximum rate of heat release (s)	Average rate of heat release (kW/m^2)	Average effective heat of combustion (MJ/kg)	Average smoke obscuration (m^2/kg)	Average carbon monoxide (kg/kg)	Average carbon dioxide (kg/kg)	Mass loss (%)
Resin									
DGEBA/DETDA	73	912.3	130	356.7	22.7	1580.9	0.0592	1.71	80.2
DGEBA/DETDA/Nano	67	762.1	130	324.1	23.5	1692.8	0.0609	1.76	80.3
DGEBA/BAPP	44	628.6	175	312.7	16.8	1064.2	0.0861	1.1	75.5
DGEBA/BAPP/Nano	55	977.2	120	448.9	20.5	1532.2	0.0876	1.51	72.2
TGDDM/DETDA	55	886.0	115	379.8	23.9	1501.9	0.0565	1.70	78.5
TGDDM/DETDA/Nano	54	1251.0	115	486.6	26.6	1371.5	0.0531	1.91	79.6
TGDDM/BAPP	44	440.9	110	140.5	11.0	723.2	0.0495	0.77	83.2
TGDDM/BAPP/Nano	42	438.5	120	198.0	18.5	1517.6	0.0828	1.20	57.2
Composite laminate									
DGEBA/DETDA	68	260.4 (1088.2)	155	175.7	22.7	1769.1	0.0555	1.68	22.0
DGEBA/DETDA/Nano	69	355.8 (1354.8)	155	210.3	23.1	1695.9	0.0575	1.73	26.9
DGEBA/BAPP	62	324.2 (1300.1)	140	182.1	21.2	1571.4	0.0869	1.63	22.9
DGEBA/BAPP/Nano	66	459.4 (1668.7)	140	226.5	21.4	1622.7	0.0949	1.64	28.9
TGDDM/DETDA	46	223.0 (928.4)	115	141.0	24.1	1716.6	0.0441	1.76	19.2
TGDDM/DETDA/Nano	52	295.4 (1203.7)	75	181.9	24.3	1643.4	0.0507	1.72	22.2
TGDDM/BAPP	32	179.9 (751.8)	60	121.7	19.7	1297.2	0.0709	1.31	15.0
TGDDM/BAPP/Nano	62	313.0 (1408.6)	95	195.2	20.7	1503.9	0.0748	1.38	21.3

[a] Values in brackets refer to heat release rates adjusted for resin content in laminate.

phosphorus containing BAPP cured systems, compared to the non-phosphorus DETDA systems. Examples of the raw data showing the level of improvement in heat release are shown in Fig. 11 for the TGDDM network and Fig. 12 for the DGEBA-based networks. The effect of BAPP compared to DETDA showed that the peak heat release rate and the average total heat release rates were reduced by 50% and 31% for the TGDDM and DGEBA networks, respectively. Smoke obscuration, CO and CO_2 outputs also showed promising improvement. The time to ignition however, for the BAPP systems was found to decrease, further underlining that the mechanism of phosphorus based systems is that degradation is promoted and the fire retardancy occurs in the condensed phase.

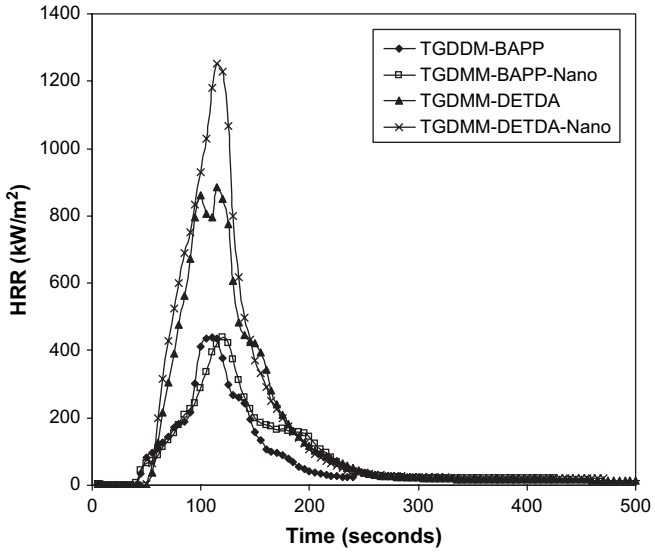

Fig. 11. Cone calorimetry data for the TGDDM resin samples showing the change in heat output during combustion.

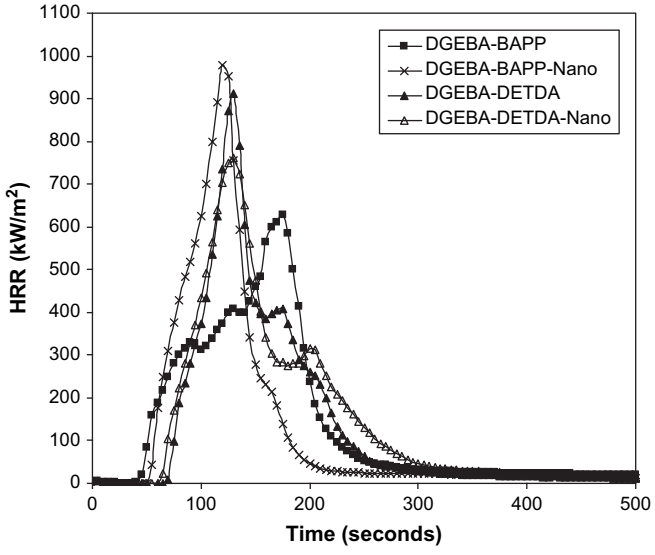

Fig. 12. Cone calorimetry data for the DGEBA resin samples showing the change in heat output during combustion.

Table 7
Comparison of char yields obtained from TGA at 850 °C, with residual mass obtained after combustion in the cone calorimeter

Sample	% Char yield at 850 °C in air (TGA)	% Char yield at 850 °C in N_2 (TGA)	% Mass after combustion (cone calorimetry)
Laminate			
DGEBA/BAPP	7.9	75.08	77.1
DGEBA/BAPP/Nano	4	72.47	71.1
DGEBA/DETDA	13.16	76.07	78
DGEBA/DETDA/Nano	2.7	72.22	73.1
Resin			
DGEBA/BAPP	4.27	27.37	24.5
DGEBA/BAPP/Nano	12.73	32.13	27.8
DGEBA/DETDA	2.95	14.02	19.8
DGEBA/DETDA/Nano	5.95	10.03	19.7
Laminate			
TGDDM/BAPP	26.32	76.07	85
TGDDM/BAPP/Nano	18.94	77.78	78.7
TGDDM/DETDA	10.39	75.98	80.8
TGDDM/DETDA/Nano	3.07	75.46	77.8
Resin			
TGDDM/BAPP	8.69	37.39	30
TGDDM/BAPP/Nano	11.51	37.42	42.8
TGDDM/DETDA	6.09	17.62	21.5
TGDDM/DETDA/Nano	6.89	23.3	20.4

Other important points to note from the resin work were that there was little evidence of any synergistic improvement via the addition of nanoclay. Apart from the nanoclay modified DGEBA/DETDA resin system, the rest of the results show either a substantial increase or else little effect upon the peak heat release rate. The larger reduction in the peak heat release rate for the TGDDM/BAPP system compared to the DGEBA/BAPP system correlates well with the increases in char yield (as determined via TGA) and increased ease of char formation (as determined by FTIR). This provides evidence for the fire retardancy mechanism occurring in the condensed phase. This correlates with the work reported by Lyon which demonstrated the close relationship between cone calorimetry and TGA char yields in a nitrogen atmosphere [32] highlighting the anaerobic environment during combustion and the role of char formation in improving fire performance.

Table 7 compares the char yields with the residual masses after combustion in cone calorimetry for all of the samples. This shows further confirmation of the relationship between the TGA and cone calorimeter char yields for both the neat resin and laminate systems. Overall the char yield at 850 °C in nitrogen compares well with the mass after combustion in the cone calorimeter (in contrast to an air atmosphere), regardless of whether the sample is a laminate or a resin plaque. While there is some scatter it is important to note the char yields from cone calorimetry for both the laminates and the neat resin systems display the same trends found in both TGA and the peak heat release rates. This further supports the role of the mechanism being related to the formation of a char layer [33], as these values correlate well with improvement in the peak heat release rates determined from cone calorimetry.

4. Conclusion

In this study the role of phosphorus within two high performance networks (TGDDM and DGEBA) has been studied using a range of techniques including XRD, TGA, FTIR, EDS and cone calorimetry. The fire retardancy mechanism has been shown to occur through the formation of a char layer which prevents the transfer of combustible products. The char was shown to form through initial cleavage of P–O–C bonds prior to scission of other covalent bonds, followed by dehydration, and subsequent charring during decomposition. TGA showed that the decomposition process formed stable char in non-oxidative environments, becoming more complex and less thermally stable in oxidative environments. TGA also highlighted the decrease in thermal stability of the networks, during initial degradation while increasing the thermal stability of the char layer. TGA showed that the laminated systems did not show a significant difference to the neat resin systems, with respect to the initial decomposition of the network and the thermal stability of the char layer.

Cone calorimetry also indicated substantial improvements in fire performance for the BAPP systems compared to the DETDA systems as determined using this technique. A strong correlation between char yields obtained from the TGA and the cone calorimeter data (such as the improvement in PHRRs) further supported the hypothesis that the barrier properties of the char layer provide the mechanism for improved fire retardancy. The differences between the fire performance and char yields of the TGDDM/BAPP and DGEBA/BAPP networks further reinforce this relationship. The addition of nanoclay as a nanoscale additive was not found to provide any significant, synergistic improvement in fire performance. XRD analysis however, did show that the laminate manufacture did not appear to affect the nanocomposite structure.

References

[1] Zaikov GE, Lomakin SM. Polym Degrad Stab 1996;54(2–3):223–33.
[2] Lu S, Hamerton I. Prog Polym Sci 2002;27(8):1661–712.
[3] Costes B, Henry Y, Muller G, Lindsay A, Buckingham M, Stevenson D, et al. Polym Degrad Stab 1996;54(2–3):305–9.
[4] Horold S. Int SAMPE Tech Conf 1999;31:188–97.
[5] Brown N. Reinf Plast 1999;43(10):44–50.
[6] Randoux T, Vanovervelt JC, Van den Bergen H, Camino G. Prog Org Coat 2002;45(2–3):281–9.
[7] Mikroyannidis JA, Kourtides DA. Flame-retardant composition of epoxy resins with phosphorus compounds. In: Advances in chemistry series, vol. 208. Oxford Univ Press; 1984. p. 351–6.
[8] Chin WK, Shau MD, Tsai WC. J Polym Sci Polym Chem Ed 1995;33: 373–9.
[9] Levchik SV, Camino G, Costa L, Luda MP. Polym Degrad Stab 1996; 54(2–3):317–22.
[10] Lin CH, Wang CS. Polymer 2001;42(5):1869–78.
[11] Derouet D, Morvan F, Brosse JC. J Appl Polym Sci 1996;62:1855–68.
[12] Tchatchoua C, Ji Q, Srinivasan SA, Ghassemi H, Yoon TH, Martinez-Nunez M, et al. Polym Prepr (Am Chem Soc Div Polym Chem) 1997; 38:113–4.
[13] Green J. Fire Mater 1995;19(5):197–204.
[14] Green J. Polym Degrad Stab 1996;54(2–3):189–93.
[15] Bellenger V, Fontaine E, Fleishmann A, Saporito J, Verdu J. Polym Degrad Stab 1984;9(4):195–208.
[16] Grassie N, Guy MI, Tennent NH. Polym Degrad Stab 1985;13(1): 11–20.
[17] Rose N, Le Bras M, Delobel R, Costes B, Henry Y. Polym Degrad Stab 1993;42(3):307–16.
[18] Liu YL, Hsiue GH, Lan CW, Chiu YS. Polym Degrad Stab 1997;56(3): 291–9.
[19] Troitzsch JH. Prog Org Coat 1983;11(1):41–69.
[20] Hergenrother PM, Thompson CM, Smith JG, Connell JW, Hinkley JA, Lyon RE, et al. Polymer 2005;46:5012–24.
[21] Hsiue G-H, Liu Y-L, Tsiao J. J Appl Polym Sci 2000;78:228–35.
[22] Liu YL, Chiu YC, Wu CS. J Appl Polym Sci 2003;87(3):404–11.
[23] Bourbigot S, Le Bras M, Dabrowski F, Gilman JW, Kashiwagi T. Fire Mater 2000;24(4):201–8.
[24] Chiang CL, Ma CCM, Wang FY, Kuan HC. Eur Polym J 2003;39(4): 825–30.
[25] Wang DY, Wang YZ, Wang JS, Chen DQ, Zhou Q, Yang B, et al. Polym Degrad Stab 2005;87(1):171–6.
[26] Chigwada G, Wilkie CA. Polym Degrad Stab 2003;81(3):551–7.
[27] Liu W, Varley RJ, Simon GP. J Appl Polym Sci 2004;92(4):2093–100.
[28] Becker O, Cheng YB, Varley RJ, Simon GP. Macromolecules 2003; 36(5):1616–25.
[29] Rose N, Le Bras M, Bourbigot S, Delobel R, Costes B. Polym Degrad Stab 1996;54(2–3):355–60.
[30] Levchik SV, Camino G, Luda MP, Costa L, Costes B, Henry Y, et al. Polym Degrad Stab 1995;48(3):359–70.
[31] Camino G. Intumescent fire retardant epoxy resins, Additives '98, 7th international conference and exhibition. Society of Plastic Engineers (SPE); 1998. p. 1/1–6.
[32] Lyon RE. Fire Mater 2000;24:179–86.
[33] Price D, Bullett KJ, Cunliffe LK, Hull TR, Milnes GJ, Ebdon JR, et al. Polym Degrad Stab 2005;88(1):74–9.